

# **Ultrafast All-optical Switches Based on Intersubband Transitions in GaN/AlN Multiple Quantum Wells for Tb/s Operation**

Jahan M. Dawlaty, Farhan Rana and William J. Schaff

Department of Electrical and Computer Engineering, Philips Hall, Cornell University, Ithaca, NY 14853, U.S.A

(Award for Best Paper)

**Proceedings of the Fall Meeting of the Materials Research Society, 2004**

## **ABSTRACT**

Theoretical and experimental results on ultra-fast all-optical switches based on intersubband transitions for Tb/s operation are presented. Designs for engineering intersubband transitions (ISBT) in GaN/AlN quantum wells near communication wavelengths ( $\sim 1.55 \mu\text{m}$ ) and for realizing all-optical switches requiring small pulse energies are discussed. Optimized designs show all-optical switching at Tb/s data rates with pulse energies as small as 200 fJ. Experimental realization of narrow line-width ISBT in GaN/AlN superlattices is also demonstrated.

## **INTRODUCTION**

Ultrafast all-optical switches are expected to play an important role in high capacity optical time division multiplexed (TDM) networks. As the demand for bandwidth grows, optical networks are expected to operate at data rates approaching 1 Tb/s. Also, each channel in wavelength division multiplexed (WDM) optical network is expected to operate at data rates exceeding 100 Gb/s. At such high data rates it is desirable to perform switching entirely in the optical domain. In order to be useful in optical networks, all-optical switching devices must also require sufficiently low optical powers. All-optical switching devices based on non-resonant optical non-linearities are fast, but require large pulse energies [1] (greater than 10 pJ.) Resonant non-linearities, such as those associated with interband transitions in semiconductors, require smaller pulse energies for all-optical switching (typically less than 500 fJ) but are generally slow. For example, all-optical switches based on interband saturable absorbers and using cross-loss modulation (XLM) scheme are limited by slow carrier relaxation times to speeds not much greater than few tens of Gb/s.

All-optical switching devices for operation at data rates close to 1 Tb/s need to be able to restore their state in time periods smaller than 1 ps. It is well known that electron intersubband relaxation times in semiconductor quantum wells are around 1 ps or less, and are three orders of magnitude smaller than interband relaxation times ( $\sim 1 \text{ ns}$ ) [2,3]. These fast relaxation times can be used to realize ultrafast all-optical switches. Intersubband devices such as quantum cascade lasers (QCL), and intersubband quantum well infrared photodetectors (QWIP) have been developed by many groups [2-5]. However, these devices do not utilize the fast intersubband relaxation times for ultra-fast applications and mostly operate at wavelengths much longer than the communication wavelength (larger than  $3 \mu\text{m}$ ). Semiconductor heterostructures with large conduction band offsets, such as GaN/AlGaN/AlN, are required for realizing intersubband transitions at communication wavelengths ( $\sim 1.55 \mu\text{m}$ ). In this paper, results on all-optical waveguide switches based on cross-loss modulation in GaN/AlN quantum wells are presented.

## ELECTRON ENERGY LEVELS IN GAN/ALN QUANTUM WELLS

In this Section, theoretical results for the electron energy levels in the conduction band of GaN/AlN superlattices are presented. The calculations are based on self-consistent solutions of Shrodinger and Poisson equations and also take into account the large spontaneous and piezoelectric polarization fields present in Nitride quantum wells. The parameters for the alloy AlGaN unless stated otherwise are obtained via linear interpolation from the values given below in table I.

**Table. I.** GaN and AlN properties used in calculations.

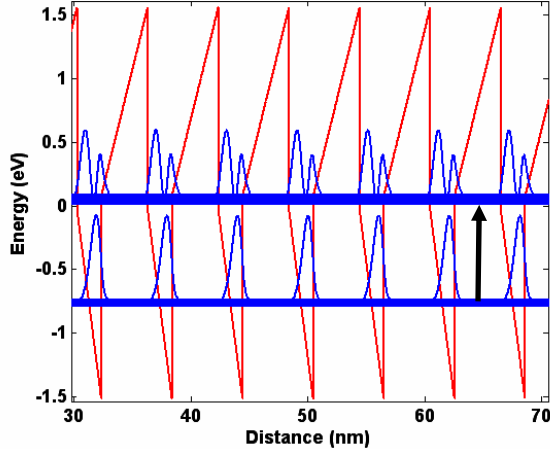
Parameters	GaN	AlN
Lattice constant (A°): a C	3.189 5.185	3.112 4.982
Band gap (eV)	3.45	6.2
$m_{\text{eff}}(m_e)$	0.23	0.30
$\epsilon_r$	9.2	8.5
Polarization (C/m <sup>2</sup> ): Spontaneous Piezoelectric	-0.029 -1.36	-0.081 -1.72
Elastic constants (GPa) : C <sub>11</sub> C <sub>12</sub> C <sub>13</sub> C <sub>33</sub>	390 145 106 398	410 148 99 388

The quantum wells are assumed to be n-doped with a density of  $10^{18}\text{cm}^{-3}$ . Figure 1 shows the electron wave-functions for the first two subbands and the conduction band profile for a superlattice with 8 monolayer (ML) GaN wells and 16 monolayer (ML) AlN barriers. The dependence of the intersubband transition energy (expressed in wavelength) on the thicknesses of quantum wells and barriers in a GaN/AlN superlattice is shown in figure 2. The steep slope of the lines indicate that even one monolayer variation in the quantum well thickness can shift the transition energy by more than 200 nm. The change in transition energy with barrier thickness is less drastic - especially for the wider quantum wells. In order to achieve intersubband transitions near  $1.55\text{ }\mu\text{m}$  in 7, 8 and 9 ML quantum wells, the required barrier thicknesses are found to be 6, 16 and 25 ML, respectively, and the required Al fractions in the  $\text{Al}_x\text{Ga}_{1-x}\text{N}$  buffer layer for stress-free growth [6] of these superlattices are  $x = 0.48, 0.68$  and  $0.75$ , respectively.

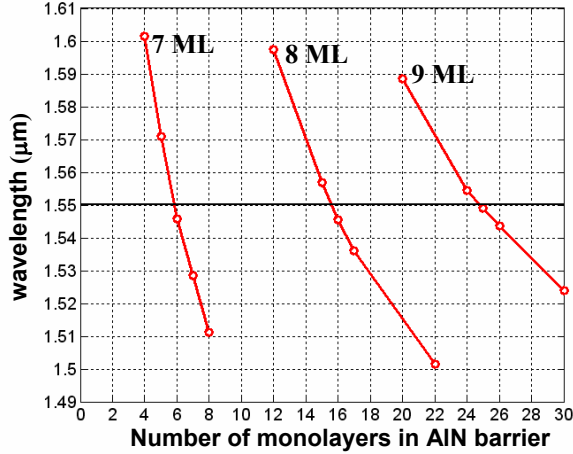
## EXPERIMENTAL RESULTS

Figure 3 shows the measured intersubband absorption spectrum of a 20 period GaN/AlN superlattice. The material growth was done with molecular beam epitaxy (MBE). For the measurements a rectangular piece of the sample ( $\sim 1\text{cm} \times 0.5\text{ cm}$ ) was angle-polished (see inset of figure 3) and a Fourier Transform Infrared (FTIR) spectrometer was used to obtain the absorption spectrum. Light polarization was selected with two Glan-Thompson calcite polarizers both before and after the sample. Figure 3 shows the absorption spectrum for s-polarization. The wavelength of the absorption peak corresponds to a superlattice with 7 ML GaN wells and 22 ML AlN barriers. The length of one period (73 A°) matches well with the periodicity of the

structure measured by small-angle X-ray diffraction ( $74.2 \text{ \AA}^\circ$ ). The small absorption linewidth (130 nm) indicates excellent growth uniformity. As mentioned earlier, one monolayer variation in the well thickness can result in inhomogenous linewidths wider than 200 nm.



**Figure 1.** Conduction band profile and magnitudes of electron wavefunctions in a superlattice of 8 ML GaN wells and 16 ML AlN barriers. The transition is shown by the arrow.



**Figure 2.** Intersubband transition energies (expressed in wavelengths) for three widths of GaN quantum wells (three lines) versus number of monolayers in AlN barriers.

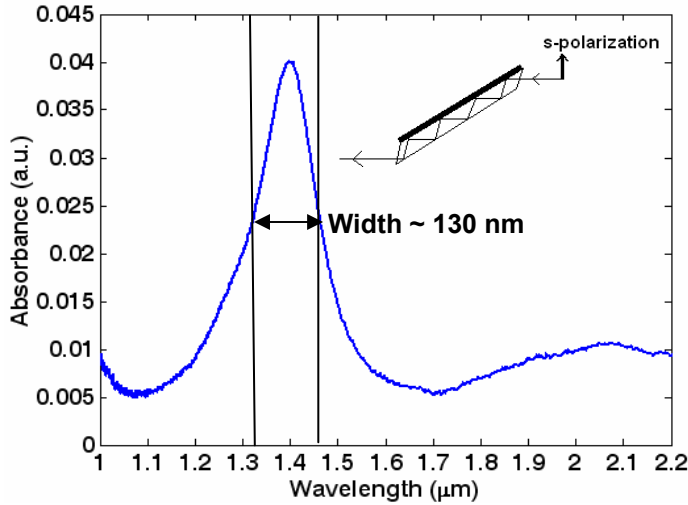


**Figure 3.** Polarization dependant absorption of a 7 ML GaN quantum well and 22 ML AlN barrier superlattice grown on sapphire.

## ALL-OPTICAL SWITCHING CHARACTERISTICS

The cross-loss modulation (XLM) scheme for all-optical switching is shown in figure 4. Both the data pulse and the control pulse are coupled into a saturable absorber. In the absence of the control pulse, the data pulse is absorbed in the device. The control pulse, when present, saturates the loss of the absorber and allows the data pulse, traveling with the control pulse, to be transmitted through the device. Here, we discuss the characteristics of GaN /AlN intersubband saturable absorbers for all-optical switching. The transverse cross-section of a typical device is

shown in figure 5. The equations for the pulse intensity  $I(z,t)$  and carrier densities in the lower and upper energy levels,  $N_2(z,t)$  and  $N_1(z,t)$ , respectively, are:

$$\frac{dN_2(z,t)}{dt} = -\frac{N_2(z,t)}{\tau_r} - (N_2(z,t) - N_1(z,t)) \frac{I(z,t)}{E_{sat}} \quad (1a)$$

$$\frac{dN_1(z,t)}{dt} = -\frac{dN_2(z,t)}{dt} \quad (1b)$$

$$\frac{\partial I(z,t)}{\partial z} + \frac{1}{v_g} \frac{\partial I(z,t)}{\partial t} = \hbar\omega_0 A (N_2(z,t) - N_1(z,t)) \frac{I(z,t)}{E_{sat}} \quad (1c)$$

where,  $\tau_r$  is the intersubband relaxation time,  $E_{sat}$  is the saturation energy,  $\hbar\omega_0$  is the photon energy, and  $A$  is the sum of the cross-sectional areas of all quantum wells (active area).

The saturation energy  $E_{sat}$ , can be calculated from the relation [3] ,

$$E_{sat} = \hbar\omega_0 \frac{A}{\Gamma} \left( \frac{\epsilon_0 n_{eff} \lambda_0 \hbar \gamma}{2 \pi e^2 z_{21}^2} \right) \quad (2)$$

where,  $\Gamma$  is the confinement factor of the transverse optical mode in the active area. The ratio  $A/\Gamma$  is the effective area of the optical mode ( $A_{eff}$ ).  $\epsilon_0$ ,  $n_{eff}$ ,  $\lambda_0$  and  $e$  are the vacuum permittivity, mode effective index, wavelength of light and the electron charge, respectively.  $2\hbar\gamma$  is the homogeneous linewidth. of the transition.  $z_{21}$  is the optical dipole matrix element between the lower and upper energy levels. In order to achieve XLM with very low control pulse energies, one needs to minimize  $E_{sat}$ . Minimization of the saturation energy is accomplished by choosing superlattices with large confinement factors  $\Gamma$  and dipole matrix elements  $z_{21}$ , while keeping the active area  $A$  of the device small.

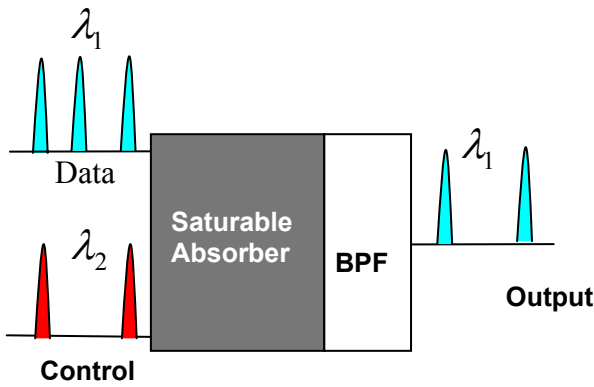


**Figure 4.** Schematic diagram of all-optical switching with a saturable absorber. The control pulse with wavelength  $\lambda_2$  is filtered out of the output channel with the band -pass filter (BPF.)

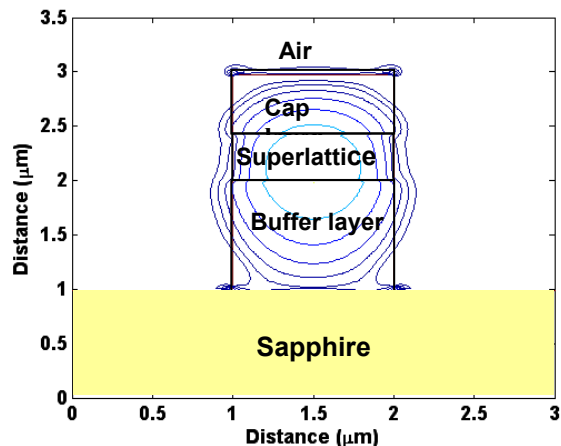


**Figure 5.** The contour of the fundamental transverse optical mode superimposed on the cross-section of a typical wave-guide.

The superlattice structure is typically grown on a fully relaxed AlGaN buffer layer. In order to obtain a defect free fully relaxed AlGaN buffer layer, the thickness of the buffer layer must be at least 0.5-1.0  $\mu\text{m}$ . However, a thick buffer layer results in reduced confinement of the optical mode in the superlattice. The calculated saturation energies for different device structures are shown in figures 6. In figure 6.a and figure 6.b the buffer layer thicknesses are assumed to be

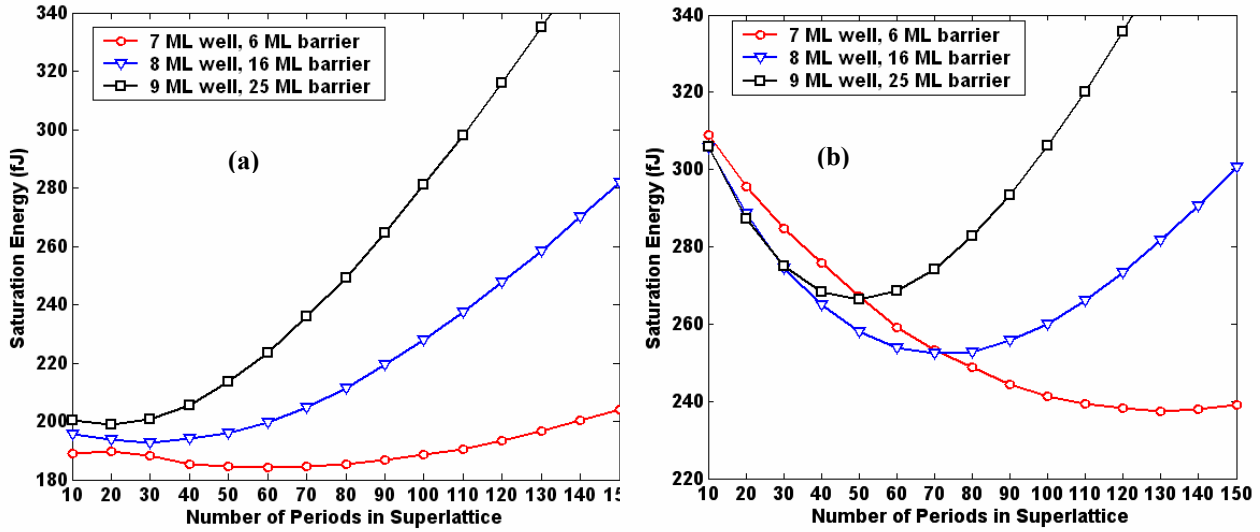


**Figure 6.** Pulse saturation energies for two choices of buffer layer thickness: (a) 0.5  $\mu\text{m}$  and (b) 1.0  $\mu\text{m}$ . Different lines correspond to various choices of well and barrier thicknesses in monolayers (ML) for 1.55  $\mu\text{m}$  intersubband transition.

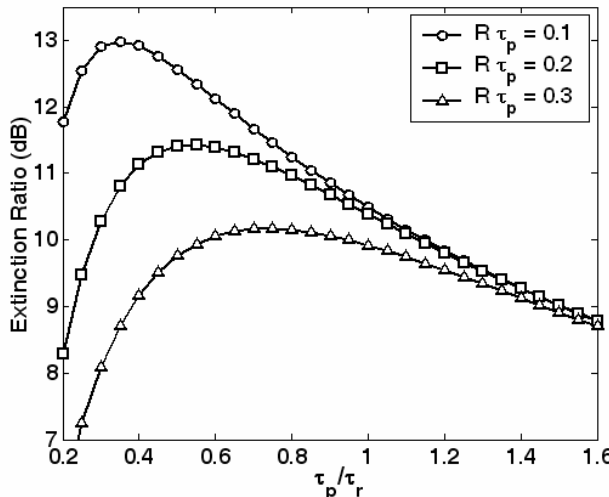


**Figure 7.** Extinction ratio for the output signal pulses as a function of the ratio between the control pulse width  $\tau_p$  and relaxation time  $\tau_r$  for different values of the product of data rate  $R$  (bits/s) and  $\tau_p$ . Relaxation time of  $\tau_r = 200$  fs, control pulse energy of 600 fJ, data pulse energy of 50 fJ and saturation energy 200 fJ were assumed.

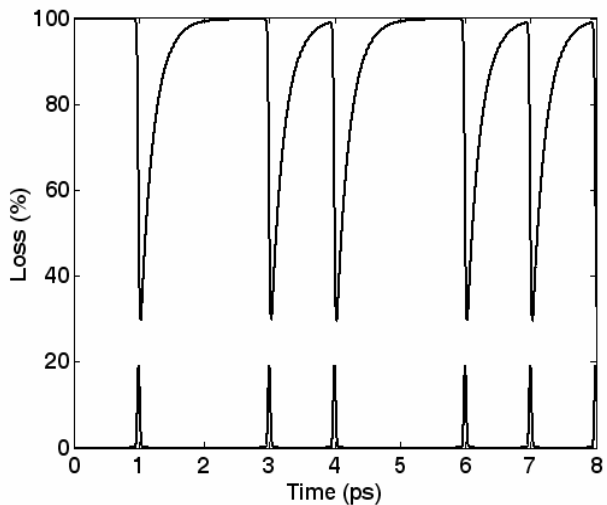


**Figure 8.** Loss saturation caused by a random control pulse sequence (with 600 fJ energy per pulse) in intersubband saturable absorber with saturation energy of 200 fJ. Relaxation time is  $\tau_r = 200$  fs and pulse width  $\tau_p$  is set to 0.35  $\tau_r$ .

0.5  $\mu\text{m}$  and 1.0  $\mu\text{m}$ , respectively. In calculating the saturation energies, 50 nm homogenous linewidth and 1.0  $\mu\text{m}$  wide waveguides were assumed. In the optical mode simulations the refractive index of  $\text{Al}_x\text{Ga}_{1-x}\text{N}$  was assumed to be given by the empirical relation [7]:

$$n(\text{Al}_x\text{Ga}_{1-x}\text{N}) = 0.431 x^2 - 0.735 x + 2.335 \quad (3)$$

The thickness of the cap layer for each point in figure 6 is optimized for maximum optical confinement in the active region. The minimum saturation energies for a 0.5  $\mu\text{m}$  thick buffer layer (figure 6.a) are between 190 – 200 fJ.

Device performance was simulated by numerically solving equations 1 using the split-step Fourier method [8,9]. Figure 7 shows that extinction ratios between logical 1 and logical 0 higher than 10 dB can be achieved at data rates faster than  $R = 1 \text{ Tb/s}$  and control pulse energies of 600 fJ. Figure 8 shows that loss saturation in the device is bit-pattern independent. Using control pulse energies as low as 200 fJ results in extinction ratios of about 5 dB.

## CONCLUSION

We have calculated design parameters for GaN/AlN superlattices for realizing intersubband devices operating at communication wavelengths ( $\sim 1.55 \mu\text{m}$ ). The experimental measurements show good agreement with theoretical calculations. We also presented design considerations for all-optical intersubband switches using XLM with low pulse switching energies. All-optical switches based on intersubband transitions in GaN/AlN superlattices can operate with control pulse energies as small as 200 fJ.

## ACKNOWLEDGEMENT

We gratefully acknowledge the research division of Corning Inc. for sharing their FTIR spectrometer. We also acknowledge support from NSF.

## REFERENCES

1. J. P. Skoloff, P. R. Prucnal, I. Glesk, M. Kane, *IEEE Photonics Tech. Letts.*, **5**, 787-790, 1993.
2. J. Faist, F. Capasso, C. Sirtori, D. L. Sivco, A. L. Hutchinson, A. Y. Cho, *Appl. Phys. Letts.*, **66**, 538-540, 1995.
3. F. Rana, R. J. Ram, *Phys. Rev. B*, **65**, 125313, 2002.
4. G. Strasser, S. Gianordoli, L. Hvozdara, W. Schrenk, K. Unterrainer, E. Gornik, *Appl. Phys. Letts.*, **75**, 1345-1347, 1999.
5. V. Ryzhii, *Intersubband infrared photodetectors*, World Scientific, NJ, USA, 2003.
6. N. J. Ekins-Daukes, K. Kawaguchi, J. Zhang, *Crystal Growth and Design*, **2** no. 4 287-292, 2002.
7. R. Hui, S. Taherion, Y. Wan, J. Li, S. X. Jin, J. Y. Lin, H. X. Jiang, *Appl. Phys. Letts.* **82**, 1326-1328, 2003.
8. G. P. Agrawal, *Nonlinear Fiber Optics*. New York: Academic, 1989, Ch. 2 and 3.
9. G.P. Agrawal, *IEEE J. Quantum Electron.* **27**, 1843-1849 (1991)